

X 1. 16



SATURN HISTORY DOCUMENT
 University of Alabama Research Institute
 History of Science & Technology Group
 Date _____ Doc. No. _____

ANALOG SIMULATION OF ^{Updated} SATURN ~~S-IB~~ ^I STAGE
 PROPULSION SYSTEM DYNAMIC CHARACTERISTICS

by
 J. W. Lehner
 Senior Engineer
 Chrysler Corporation Huntsville Operations

11/66

Analog Simulation of Saturn S-IB Stage Propulsion System Dynamic Characteristics

ABSTRACT

The purpose of this paper is to present the techniques and logic employed in the development of an analog computer model to simulate ^{Operated} Saturn IB first stage propulsion system dynamic characteristics. Restraints, problem areas, and major assumptions are included.

INTRODUCTION

The propulsion model was developed to investigate the possibility of sustained low frequency longitudinal oscillations occurring at any time during first stage powered flight of the Saturn IB. It was designed to be used in conjunction with a dynamic structural model to analyze propulsion system feed back (closed-loop) behavior. This phenomenon occurs when propellant tank fluid pressure perturbations (transmitted through the propulsion system) are sufficient to be amplified by propulsion system/structure interaction.

The propulsion system to be described is defined as the fluid-mechanical components from the propellant tank bottoms through the H-1 engines. This system is composed of eight engines (four non-gimbaled inboard engines and four gimbaled outboard engines) and sixteen feed lines (two per engine). However, only one feed line-engine system is simulated and used as representative. It is presented in two parts, feed lines and engine, to best project the methods and logic involved.

Schematics are presented which illustrate the physical characteristics of each system. Numerical designations are assigned to each liquid-mechanical line segment interface and power generating subsystem location. The resulting system subdivisions are modeled individually using their respective numerical designations as the descriptive nomenclature for model formulation.

Analytical and empirical methods are used to describe each subsystem. The lumped parameter technique is used to define fluid dynamic and turbine-turbopump dynamic characteristics. Characteristic equations simulate pump, turbine and combustion chamber steady state performance. Other specially derived techniques (not developed in this paper) are used to describe line elasticity and combustion chamber pressure time delays. These equations are then combined, in the manner illustrated in logic diagrams, to form dynamic math models of the feed lines (LOX and fuel) and engine.

System peculiarities such as pump inlet cavitation compliance, pump dynamic gain, feed line fluid-structure interconnect and combustion chamber pressure delay were investigated in separate special studies to determine their influence on system

response. These studies were performed using test methods in conjunction with computer model studies. The results were inconclusive; however, assumptions were made that reduced the effect of the resulting model deficiencies. These assumptions are delineated in the following system descriptions.

Method of Fluid-Mechanic System Analysis

The fluid-mechanical systems to be described are subdivided into individual line segments of a size less than a 30 cps one-quarter wave length to allow for an acceptable frequency response range of 0-30 cps. The location of each segment was dictated by simulation requirements. Their dynamic properties, inertance (I), capacitance (C) and resistance (R), were individually lumped as illustrated in Figure 1 to permit the following treatment.

Fluid inertance, that property of fluids which resists acceleration, appears in the general flow equation which expresses fluid flowrate (\dot{W} - lb/sec) as a function of inertance (I - sec²/in²) and the pressure differential [$(P_i - P_o - \Delta P)$ - lb/in²] available for fluid acceleration:

$$\dot{W} = \frac{1}{I} \int_{t_1}^{t_2} (P_i - P_o - \Delta P) dt = f(P_i, P_o, \Delta P, t) \quad (1)$$

Inertance is calculated using line (segment) length (L - inches), line cross-sectional area (A - in²) and the gravity constant (g = 386.4 in/sec²) as follows:

$$I = L/Ag \quad (1a)$$

A fluid flowing through a container will experience a pressure drop due to resistance resulting from fluid viscosity and/or momentum losses. The effect of this resistance (R - sec/in²) is reflected in the following equation:

$$\Delta P = f(\dot{W}_i) = R\dot{W}_i^2 \quad (2)$$

where the resistance is calculated from known flow conditions by:

$$R = \Delta P / \dot{W}_i^2 \quad (2a)$$

Capacitance is that property of a fluid-mechanical system which accounts for system elasticity. This term is a function of both fluid and container (line) elasticity. However, in most cases for this model, line influence is insignificant. The effect on system behavior is characterized by the following equation:

$$P_o = \frac{1}{C} \int_{t_1}^{t_2} (\dot{W}_i - \dot{W}_o) dt = f(\dot{W}_i, \dot{W}_o, t) \quad (3)$$

where the capacitance (C - in²) is calculated using container volume (V - in³), fluid specific weight (ρ - lb/in³) and fluid-mechanical system effective bulk modulus (β_{eff} - lb/in²) as follows:

$$C = \frac{V\rho}{\beta_{\text{eff}}} \quad (3a)$$

The term β_{eff} includes the effect of line elasticity and is determined as a function of fluid bulk modulus (β), line diameter (D = inches), line thickness (t - inches) and line modulus of elasticity (E - lb/in²) by:

$$\beta_{\text{eff}} = \frac{1}{\beta} + \frac{.87D}{Et} \quad (3b)$$

It was necessary in some cases to use effective values of inertance and capacitance due to varying segment (line) geometry. These values were calculated by dividing the segment into smaller parts, calculating the values of the respective parameters, and then combining these by the following equations to arrive at an effective magnitude:

$$C_{\text{eff}} = C_1 + C_2 + \dots + C_n \quad (4)$$

$$I_{\text{eff}} = I_1 + I_2 + \dots + I_n \quad (5)$$

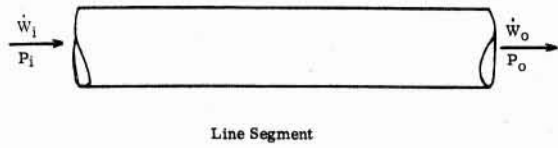
Equations 1-3 were combined for computer programming in the manner illustrated in Figure 2, to form a single segment model.

System Description

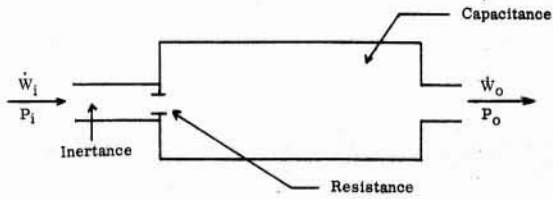
1) Feed Line Simulation

The feed lines, illustrated in Figure 3 as typical, are subject to a wide range of dynamic disturbances. All significant disturbances are expected to originate as pressure perturbations at the tank bottom. However, the complex construction (gimbal joints, expansion joint and bends) of the line exposes the fluids to various other disturbances initiated by line motion. A four segment model, illustrated in Figure 4, was developed to investigate the effects of these nebulous disturbances.

Propellant cavitation exists for some distance upstream of the pump. The degree of cavitation is dependent on pump and propellant operating conditions and is influenced by line geometry. Its effect on fluid dynamic behavior is that of a soft complex non-linear spring. This effect is simplified for simulation by assuming the cavitation bubbles to be localized at the pump inlet as a single bubble with constant linear spring characteristics. This is accomplished with capacitance C_{4-5} shown in Figure 4.



Line Segment



Line Segment Analogy

Figure 1 Typical Line Segment

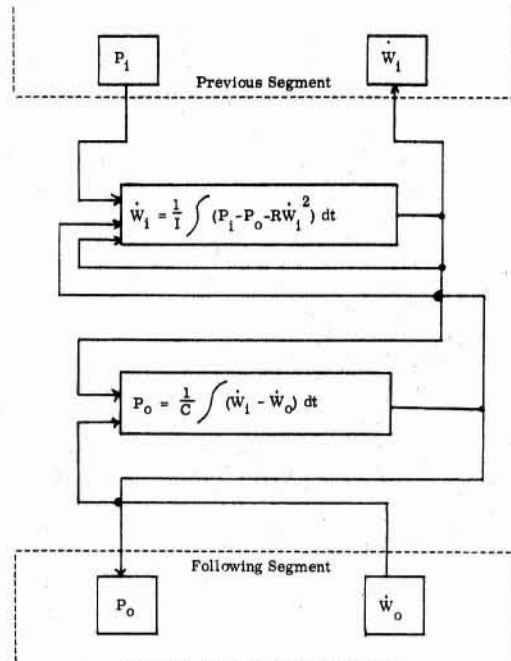


Figure 2 Single Element Simulation

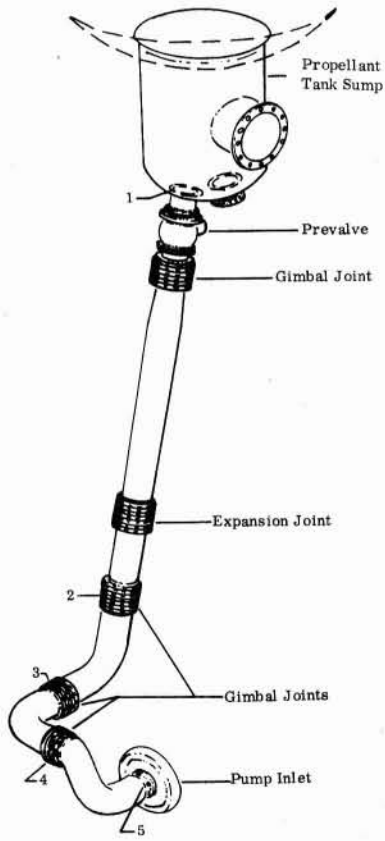


Figure 3 Typical Propellant Feed Line

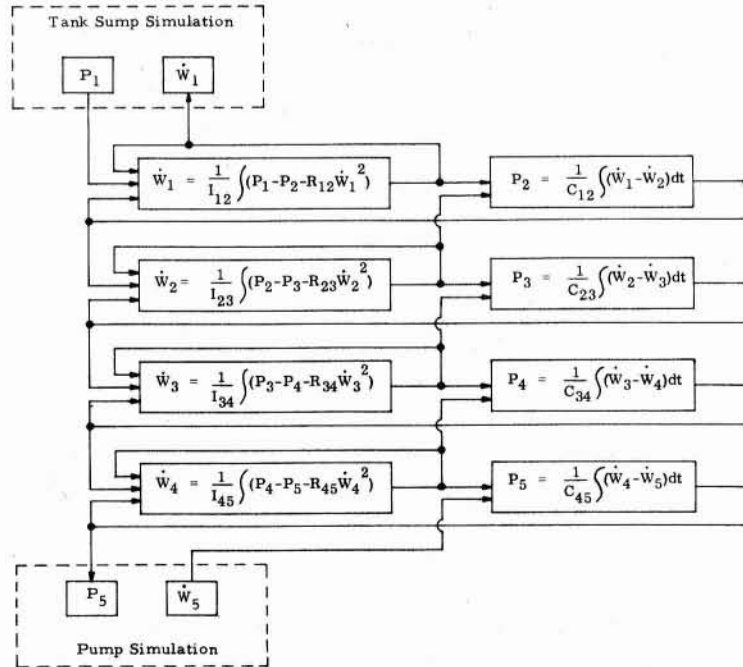


Figure 4 Typical Feed Line Simulation

The values used for C_{4-5} establish feed line resonances and correspondingly equal propulsion system resonances. This condition is illustrated in Figure 11 for a feed line resonant frequency of 15 cps.

2) Engine Simulation

The H-1 rocket engine system schematic, Figure 5, illustrates the numerical designation assigned to each liquid-mechanical segment interface and power generating subsystem (thrust chamber, etc.) location, as well as other essential engine characteristics. The system subdivisions were modeled individually using their respective numerical designation as the subscriptive nomenclature for model formulation.

As illustrated, the engine propellant flow subsystem is subdivided into LOX segments L5-6, L6-7, L8-9 and L7-10 and fuel segments F5-6, F6-7, F7-8, F8-8', F8'-9 and F7-10. These segments, with the exception of L5-6 and F5-6 (the LOX and fuel turbopumps), are modeled using the lumped parameter technique described previously. The models are then combined in the manner illustrated in Figure 7 where the inertance characteristic is represented by:

$$\dot{W} = \frac{1}{I} \int F(P, \dot{W}) dt = f(P, \dot{W}, t) \quad (6)$$

and the capacitance by:

$$P = \frac{1}{C} \int F(\dot{W}) dt = f(\dot{W}, t) \quad (7)$$

to provide the necessary flow and pressure conditions for the combustion chambers (thrust and gas generator) and pump descriptions.

The LOX and fuel turbopumps are simulated using equations derived from H-1 engine nominal steady state performance characteristic curves typically illustrated in Figure 8. These equations do not account for pump performance variation due to perturbations in inlet conditions, but are sufficient since such variations are considered small as compared to the normal operating level. The equations are of polynomial second order form and satisfactorily approximate the performance characteristics where pump pressure head (ΔP) is a function of pump flowrate (\dot{W} - lb/sec) and pump speed (\dot{N} - rpm) as follows:

$$\Delta P = f(\dot{W}, \dot{N}) = K_1 \dot{W}^2 + K_2 \dot{W} \dot{N} + K_3 \dot{N}^2 \quad (8)$$

The shaft torque required to maintain the flow conditions of equation 8 is:

$$T = f(\dot{W}, \dot{N}) = K_4 (\dot{W})(\dot{N}) / \text{Eff} \quad (9)$$

where pump efficiencies (LOX and fuel) (Eff) vary only a small amount and are usually assumed constant. K_4 is an empirical constant used to adjust the equation to any necessary condition. Equation 8 is used to derive ΔP_{L5-6} and ΔP_{F5-6} and equation 9 defines T_{L6} and T_{L7} .

Combustion chamber characteristics are derived from chamber geometry and combustion products in the form of characteristic exhaust gas velocity (C^*). This term (C^*) defines a relationship between pressure, flowrate and mixture ratio as illustrated by Figure 9 and the general rocket engine relationship

$$P_I = C^* \dot{W}_T / A_t g \quad (10)$$

in which injector end combustion pressure (P_I - psi) is a function of C^* , total flowrate (\dot{W}_T - lb/sec), chamber throat area (A_t - in²) and the gravitational constant (g - in/sec²). Steps were taken to reduce the algebraic content of the defining relationships to a minimum for analog application. In the case of the thrust chamber at a nominal mixture ratio of 2.33 pressure is predominantly a function of total propellant flowrate, and has only a minute response to expected mixture ratio changes about the nominal. For these reasons, thrust chamber steady state pressure is adequately defined by the following linear relationship:

$$P'_g = f(\dot{W}_g) = K \dot{W}_g \quad (11)$$

where K is an empirical constant and may be determined simply by

$$K = P'_g / \dot{W}_g \quad (11a)$$

Gas generator combustion performance is a strong function of both mixture ratio and total flowrate. The gas generator operates fuel rich in a region ($MR_N = .342$) well below the stoichiometric mixture ratio. As is apparent from a study of the C^* curve trend, this operating condition causes the gas generator (GG) to be exceptionally sensitive to ratio changes. Consequently, a performance perturbation (about a nominal) model of the GG was developed to enhance analog computer accuracy. The resulting equations are:

$$\Delta P_{10} = K_1 \Delta MR_{10} \dot{\Delta W}_{10} + K_2 \Delta MR_{10} + K_3 \dot{\Delta W}_{10} \quad (12)$$

$$\Delta MR_{10} = (\dot{\Delta W}_{40} + \dot{W}_{L10N}) / (\dot{\Delta W}_{F10} - \dot{W}_{F10N}) - MR_{10N} \quad (13)$$

$$\dot{\Delta W}_{10} = \dot{W}_{NF10} + \dot{W}_{NL10} - \dot{W}_{F10} - \dot{W}_{L10} \quad (14)$$

The subscript N designates nominal values of mixture ratio (MR) and flowrate (\dot{W}). Subscripts L and F represent LOX and fuel, respectively, and their omission represents a combined or total value.

Combustion delay time and chamber pressure lag time are simply represented

by a pure time delay:

$$D = f(\tau, t) = e^{-S\tau} \quad (15)$$

and a first order lag:

$$L = f(t) = \frac{1}{1 + \tau'S} \quad (16)$$

and are incorporated into equations 11 and 12 to simulate essential combustion dynamic behavior as follows:

$$P_9 = f(\dot{W}_9, D_9, L_9) = K\dot{W}_9 \left[e^{-S\tau_9/(1 + \tau'_9S)} \right] \quad (17)$$

$$\Delta P_{10} = f(\Delta MR_{10}, \Delta \dot{W}_{10}, D_{10}, L_{10}) = (K_1 \Delta MR_{10}, \Delta \dot{W}_{10} + K_2 \Delta MR_{10} + K_3 \Delta \dot{W}_{10}) \left[e^{-S\tau_{10}/(1 + \tau'_{10}S)} \right] \quad (18)$$

Values of τ' and τ are determined from propellant, chamber and operating characteristics. A constant value of τ' is used and is calculated at nominal operating conditions as:

$$\tau' = Vol/A_t v_n \quad (19)$$

where Vol is chamber volume (in³), A_t is the chamber exit throat area (in²) and v_n is the nominal gas exit velocity. A special study was performed to determine the value of τ .

Turbine operating performance is a function of inlet and outlet gas characteristics and of turbopump speed. Exit gas behavior is assumed constant for dynamic turbine operation. Turbine inlet gas characteristics, pressure, temperature, weight flowrate and inlet gas velocity are defined as functions of chamber flowrate and mixture ratio to simplify the expression for turbine torque perturbation (ΔT_{10}). These characteristics are combined with turbine hardware characteristics and turbopump speed perturbations ($\Delta \dot{N}_6$) to give:

$$\Delta T_{10} = f(\Delta \dot{W}_{10}, \Delta MR_{10}, \Delta \dot{N}_6) = K_4 \Delta \dot{W}_{10} \Delta MR_{10} + K_5 \Delta \dot{W}_{10} - \Delta \dot{N}_6 \Delta \dot{W}_{10} + K_7 \Delta MR_{10} - K_8 \dot{N}_6 \quad (20)$$

Included in the above equation is power lost due to gearbox resistance. Turbine torque is used along with total turbopump required torque (T_6) to define turbopump speed perturbations as:

$$\Delta \dot{N}_6 = \frac{1}{I_{10,6}} \int (\Delta T_{10} + T_{10N} - T_6) dt = f(\Delta T_{10}, T_6, t) \quad (21)$$

where $I_{10,6}$ is the combined inertance property of the turbopump, gearbox and turbine, and T_6 is determined from:

$$T_6 = f(T_{L6}, T_{F6}) = T_{L6} + T_{F6} \quad (22)$$

Total turbopump speed is defined as:

$$\dot{N}_6 = f(\Delta \dot{N}_6) = \dot{N}_{6N} + \Delta \dot{N}_6 \quad (23)$$

Engine thrust is determined from the general rocket engine relationship:

$$F = f(P_9) = P_9 A_9 (CF_9) \quad (24)$$

Chamber throat area ($A_9 - \text{in}^2$) and thrust coefficient (CF_9) are assumed constant.

The individual engine equations were integrated in the manner illustrated in Figure 7, to establish the engine dynamic model.

3) Propulsion System Simulation

The three models were then combined as shown in Figure 6 and programmed on an analog computer to produce single engine results which are graphically illustrated in Figures 10 and 11, as gain (dbs) versus frequency. These results were obtained to establish the individual effects of the LOX and fuel feed lines resonant conditions on propulsion response. This was accomplished by sinusoidally perturbing, separately, the LOX and fuel feed line inlets while systematically varying their respective resonant frequencies.

Propulsion system total thrust (F_T) is determined by the relationship

$$F_T = F(8) \quad (25)$$

which describes inphase engine operation, a desired worse case condition.

A more detailed description of the individual equations, along with special derivations of combustion pressure delay (\mathcal{T} , \mathcal{T}') and effective fluid bulk modulus (β_{eff}) are presented in Chrysler Technical Report No. HSM-R181.

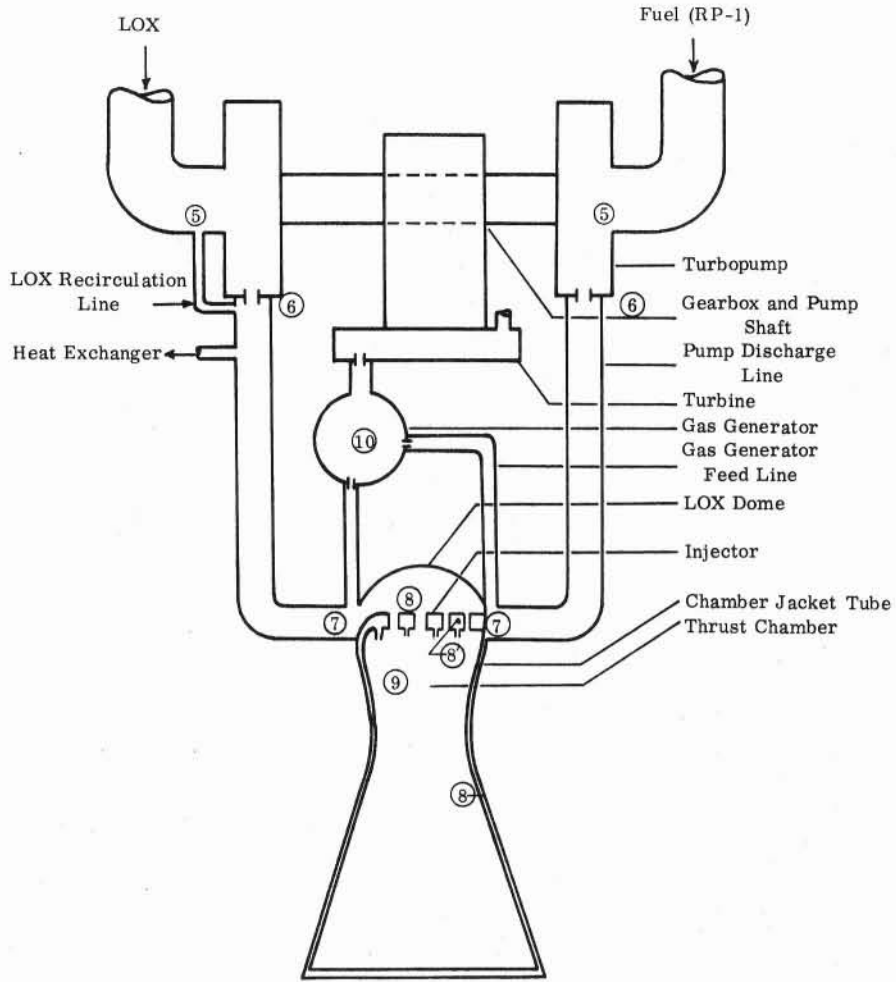


Figure 5. 200K H-1 Engine Schematic

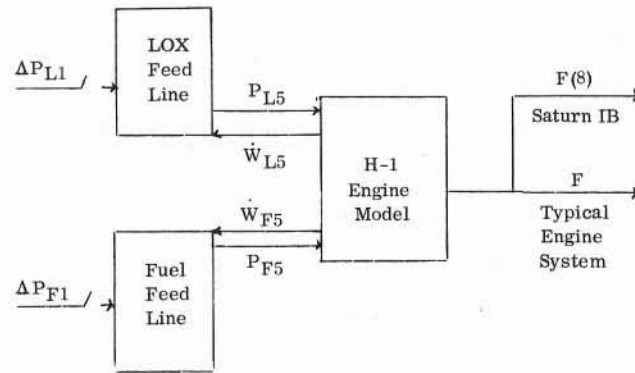


Figure 6. Propulsion System Simulation

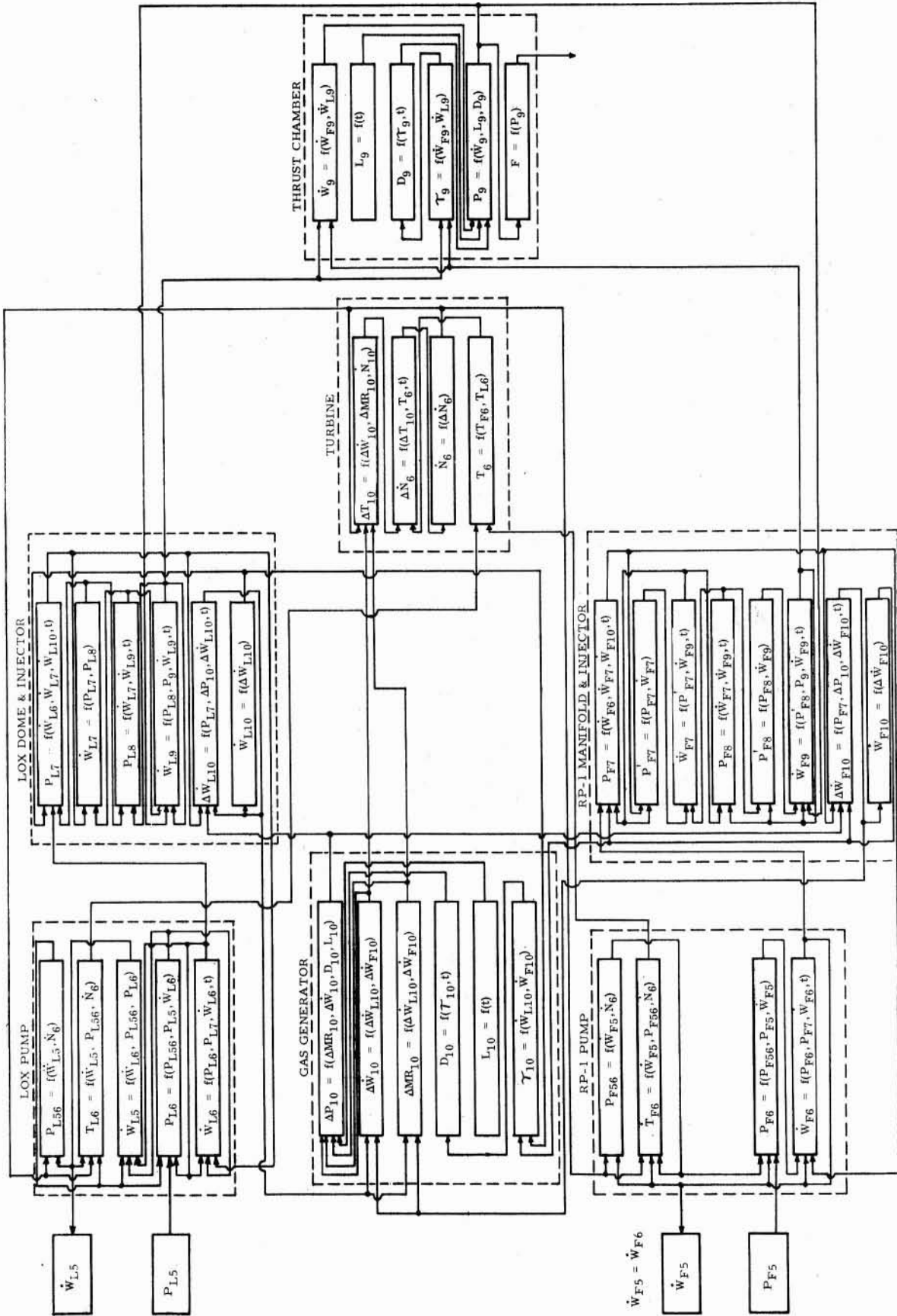


Figure 7. 200K H-1 Rocket Engine Model Logic Diagram

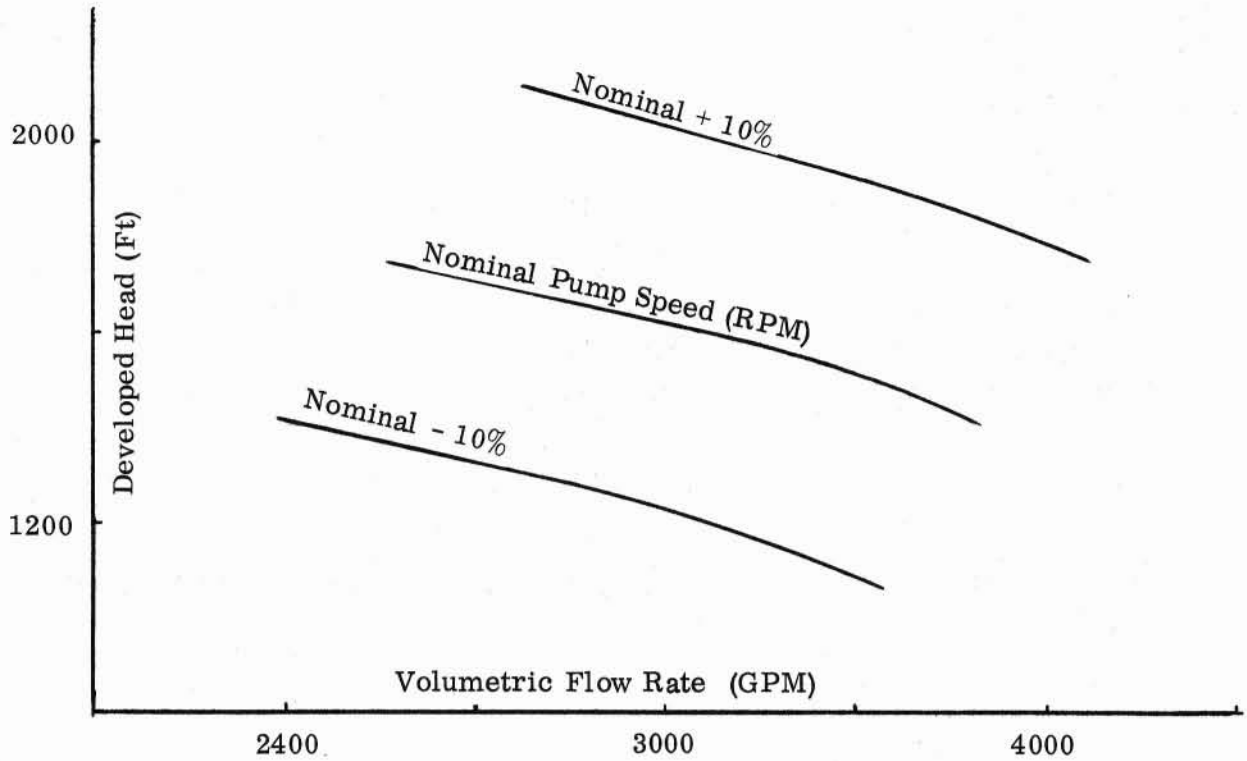


Figure 8. LOX Pump Developed Head Versus Volumetric Flow Rate and Speed

*Extracted from Rocketdyne Technical Manual No. R-1352P-3

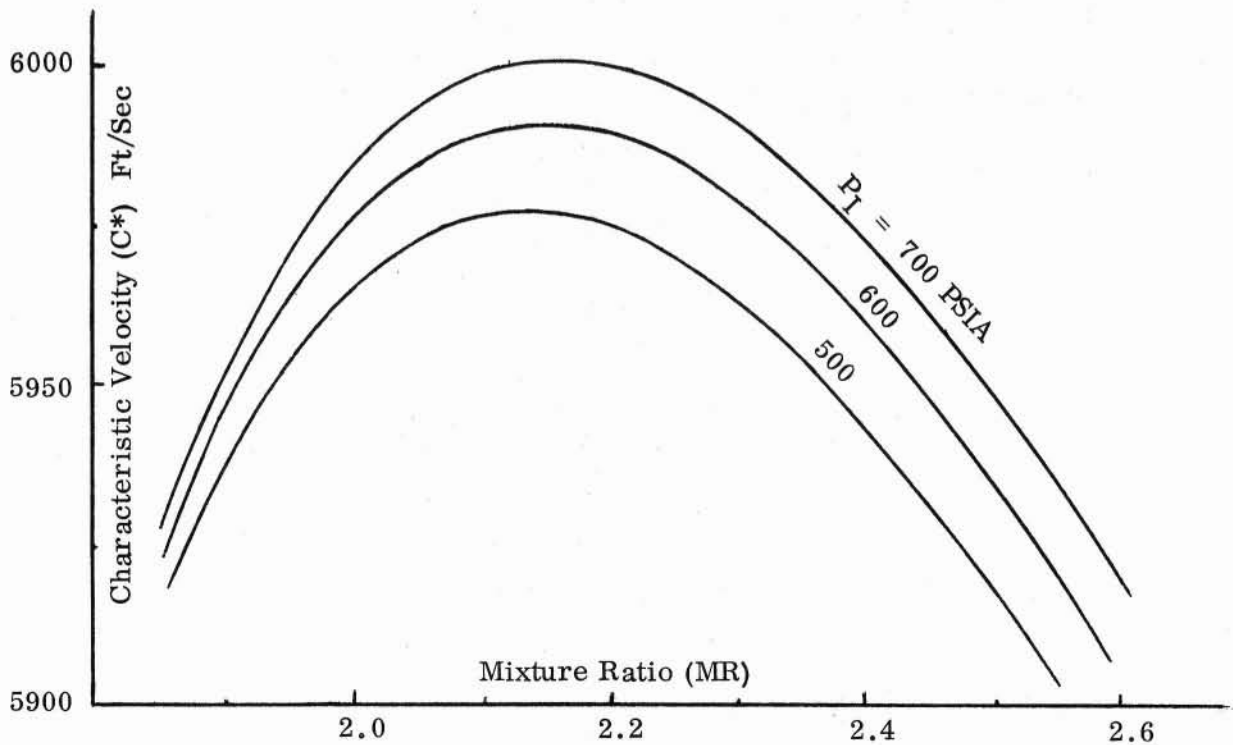


Figure 9. Characteristic Velocity Versus Injector End Chamber Pressure and Mixture Ratio

